





Communication

# Room-Temperature Synthesis of Air-Stable Near-Infrared Emission in FAPbI<sub>3</sub> Nanoparticles Embedded in Silica

Lung-Chien Chen <sup>1</sup>, Li-Wei Chao <sup>1</sup>, Chen-Yu Xu <sup>2</sup>, Chih-Hung Hsu <sup>3</sup>, Yi-Ting Lee <sup>4</sup>, Zi-Min Xu <sup>1</sup>, Chun-Cheng Lin <sup>5,\*</sup> and Zong-Liang Tseng <sup>2,\*</sup>

<sup>1</sup> Department of Electro-Optical Engineering, National Taipei University of Technology, Taipei 106344, Taiwan; ocean@ntut.edu.tw (L.-C.C.); aa0932693328@gmail.com (L.-W.C.); eok26732687@gmail.com (Z.-M.X.)

<sup>2</sup> Department of Electronic Engineering, Ming Chi University of Technology, New Taipei City 24301, Taiwan; u06157020@mail2.mcut.edu.tw

<sup>3</sup> Giant-Tek Corporation, Miaoli County 35048, Taiwan; rex@giant-tex.com.tw

<sup>4</sup> Center for Organic Photonics and Electronics Research (OPERA), Kyushu University, 744 Motooka, Nishi, Fukuoka 819-0395, Japan; ytleee@opera.kyushu-u.ac.jp

<sup>5</sup> Department of Mathematic and Physical Sciences, General Education, R.O.C. Air Force Academy, Kaohsiung 82047, Taiwan

\* Correspondence: cclincafa@gmail.com (C.-C.L.); zltseeng@mail.mcut.edu.tw (Z.-L.T.)

**Abstract:** Hybrid organic–inorganic and all-inorganic metal halide perovskite nanoparticles (PNPs) have shown their excellent characteristics for optoelectronic applications. We report an atmospheric process to embed formamidinium CH(NH<sub>2</sub>)<sub>2</sub>PbI<sub>3</sub> (FAPbI<sub>3</sub>) PNPs in silica protective layer at room temperature (approximately 26 °C) employing (3-aminopropyl) triethoxysilane (APTES). The resulting perovskite nanocomposite (PNCs) achieved a high photoluminescence (PL) quantum yield of 58.0% and good stability under atmospheric moisture conditions. Moreover, the PNCs showed high PL intensity over 1 month of storage (approximately 26 °C) and more than 380 min of PNCs solutions in DI water. The studied near-infrared (NIR) light-emitting diode (LED) combined a NIR-emitting PNCs coating and a blue InGaN-based chip that exhibited a 788 nm electroluminescence spectrum of NIR-LEDs under 2.6 V. This may be a powerful tool to track of muscle and disabled patients in the detection of a blood vessel.

**Keywords:** perovskite; nanocrystals; APTES; CH(NH<sub>2</sub>)<sub>2</sub>PbI<sub>3</sub>; FAPbI<sub>3</sub>; NIR



**Citation:** Chen, L.-C.; Chao, L.-W.; Xu, C.-Y.; Hsu, C.-H.; Lee, Y.-T.; Xu, Z.-M.; Lin, C.-C.; Tseng, Z.-L.

Room-Temperature Synthesis of Air-Stable Near-Infrared Emission in FAPbI<sub>3</sub> Nanoparticles Embedded in Silica. *Biosensors* **2021**, *11*, 440. <https://doi.org/10.3390/bios11110440>

Received: 13 September 2021

Accepted: 3 November 2021

Published: 4 November 2021

**Publisher's Note:** MDPI stays neutral with regard to jurisdictional claims in published maps and institutional affiliations.



**Copyright:** © 2021 by the authors. Licensee MDPI, Basel, Switzerland. This article is an open access article distributed under the terms and conditions of the Creative Commons Attribution (CC BY) license (<https://creativecommons.org/licenses/by/4.0/>).

## 1. Introduction

Organic–inorganic Formamidinium lead halide (CH(NH<sub>2</sub>)<sub>2</sub>PbX<sub>3</sub> or FAPbX<sub>3</sub>, X = Cl, Br, I) perovskite nanoparticles (PNPs) have been regarded as novel materials for many optoelectronic applications owing to their advanced class of direct bandgap and excellent photophysical properties, such as strong absorption coefficient, narrow emission width, ease of size control, and so on [1–7]. The applications of such PNPs have also been shown in different fields, including solar cells [8], sensitive photodetectors [9–13], low threshold lasers [14,15], laser diodes [16], and light emitting diodes [16–18]. Compared to the all-inorganic Cs- or organic–inorganic CH<sub>3</sub>NH<sub>3</sub>-based PNPs, the organic–inorganic formamidinium-based PNPs have higher stability such as higher chemical, thermal, and moisture stability [15,19–24]. Nevertheless, the poor stability of organic–inorganic hybrid perovskites against oxygen, water, and thermal treatment has restricted their actual applications [25].

Several methods were presented to improve the stability of the PNPs. For example, enclosing PNPs in poly (methyl methacrylate) [26,27], polyhedral oligomeric silsesquioxane (POSS) [28] and inorganic SiO<sub>2</sub> network structure were used to effectively keep optical and chemical stabilities of the PNPs. Compared with the organic encapsulation coating, the inorganic SiO<sub>2</sub> encapsulation was widely used to prevent the influence of atmospheric moisture and oxygen for PNPs [29,30]. In addition, silica-wrapped PNPs could be applied

in phosphor powders and light conversion films to exchange the light-emitting color. Hu et al., reported the silica-coated process to encapsulate CdSe/ZnS QDs in 2009 [31], but silica-coated CsPbX<sub>3</sub> (X = Cl, Br and I) PNPs compounds were fabricated until 2016 [32,33]. Subsequently, APTES [34–36], tetraethylorthosilicate (TEOS), and Tetramethoxysilane (TMOS) were utilized to form silica-coated CsPbX<sub>3</sub> (X = Cl, Br and I) PNPs.

The PNPs were synthesized by a typical hot injection process and a post treatment for encapsulation, which exhibits a low throughput. Sun and coworkers used a one-pot method to prepare silica-coated CsPbX<sub>3</sub> (X = Cl, Br and I) PNP, which added a little number of APTES during the hot injection process. This is an easy and effective method to improve stability [34]. Organic–inorganic CH<sub>3</sub>NH<sub>3</sub>PbBr<sub>3</sub> PNPs were also prepared in a facile room-temperature one-pot method employing (3-aminopropyl) trimethoxysilane (APTMS) [37], which ensures high luminescence and stability using an easy and rapid strategy. It is highly desirous to develop a near-infrared (NIR) light for the tracking of muscle or disabled patients in the detection of blood vessel, because 650–950 nm wavelengths in NIR are less significantly absorbed by human skin, and can therefore penetrate deeper into the body [38]. Therefore, a one-pot method is necessary for silica-wrapped NIR FAPbI<sub>3</sub> PNPs at room temperature in open air.

Herein, a fast, simple, and efficiency strategy to synthesize high-stability PNPs embedded into silica by air synthesis at room temperature was demonstrated. The perovskite nanocomposites (PNCs) were prepared via a APTES hydrolysis encapsulation strategy. The NIR PNCs was very stable in several rigorous conditions, such as storing in the humid air and ultrasonication in water. In addition, NIR-LED devices were also prepared by FAPbI<sub>3</sub> PNCs as the light-conversion materials coated on the commercial blue InGaN chip. The PNCs exhibits well moisture-resistant and air stability with a long operating lifetime compared to FAPbI<sub>3</sub> PNPs.

## 2. Materials and Methods

### 2.1. Air-Synthesis of NIR-FAPbI<sub>3</sub> PNPs and PNCs

First, 0.1 mmol of formamidine acetate (99%) was dissolved in 10 mL OCTA and stirred 10 min at room temperature (25 °C) in open air for preparation FA precursor as the first step. Then, 0.1 mmol of lead (II) iodide (PbI<sub>2</sub>, 99.999%) were dissolved in a mixture of 10 mL of toluene (98%), 0.8 mL of oleic acid (OA, 90%), 1.2 mL of oleylamine (OAM, 90%), and 1 mL of APTES (99%) at room temperature in the air under stirring for 1 h until PbI<sub>2</sub> was completely dissolved. Subsequently, 2 mL of FA precursor solution was added into the mixture and vigorously stirred for 30 min. The mixture solution was added to hexane (95%) and centrifuged at 9000 rpm for 5 min and the hexane was used to disperse the precipitates. After the second centrifugation, the powders of the NIR-FAPbI<sub>3</sub> PNCs can be obtained by removing the hexane under the airflow at room temperature.

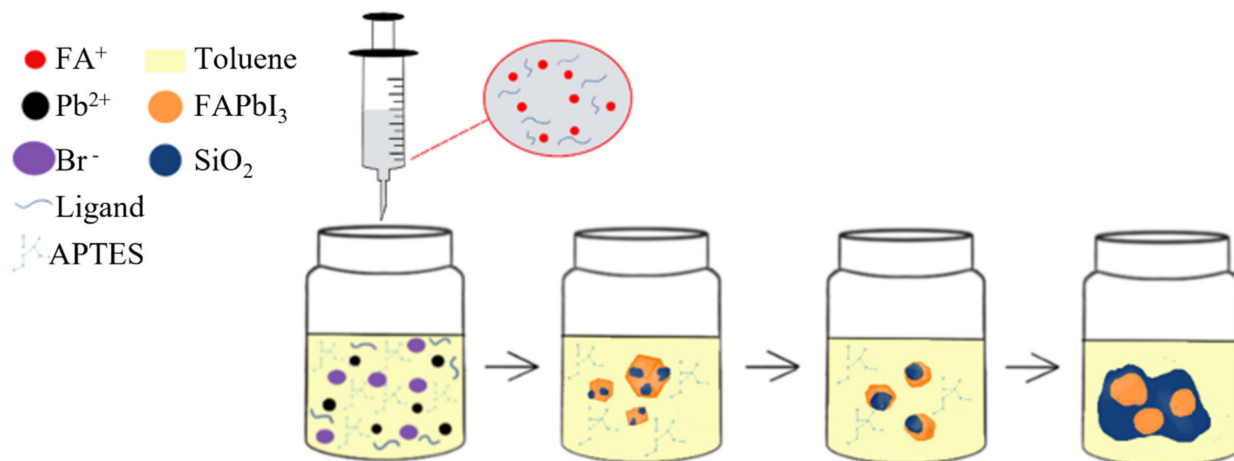
### 2.2. Manufacture of NIR-LEDs and Characterization

The NIR-FAPbI<sub>3</sub> NCs powders and the UV resin (weight ratio = 1:2) were mixed, coated on blue LED chips (wavelength = 455 nm), and baked at 70 °C for 5 min in an oven. Consequently, UV curing for 30 s in air used a 365 nm UV lamp to obtain the color-converted layers. Electroluminescence (EL) performances were measured using an LQ-100R spectrometer (Enlitech, Kaohsiung, Taiwan). Photoluminescence quantum yield (PLQY) and photoluminescence (PL) were obtained using F-7000 (Hitachi, Tokyo, Japan). The surface morphologies of samples were observed using JEM-2100 (JEOL, Tokyo, Japan) and JSM-7610F (JEOL). FTIR spectra was measured using spectrum one (PerkinElner, Waltham, MA, USA). X-ray diffractometer (XRD) patterns were measured using a D8 ADVANCE (Bruker, Billerica, MA, USA).

## 3. Results and Discussion

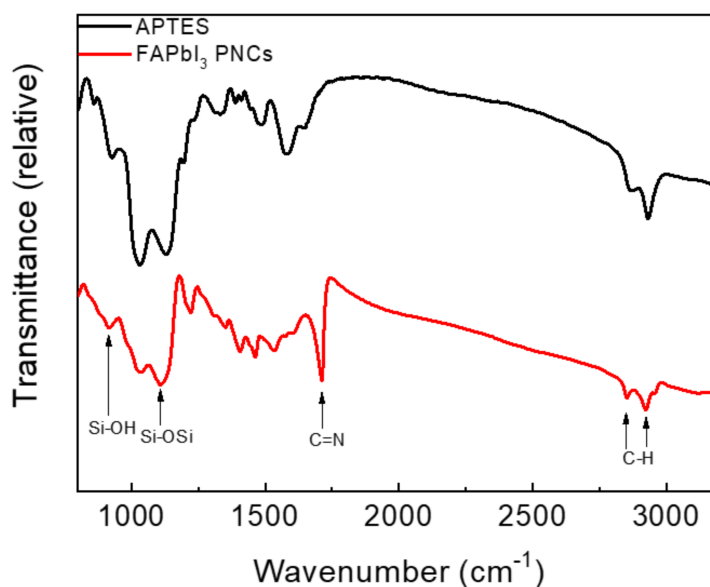
PNCs were obtained through the air synthesis at room temperature. The simple reaction system, PbI<sub>2</sub>, OA, OAM, toluene, and APTES in one pot, was stirred 30 min at

room temperature (28 °C) in open air (Figure 1). The FA precursor was then rapidly injected into the mixture, and the colorless solution turned dark red immediately, which indicates the constitution of FAPbI<sub>3</sub> PNCs (Video S1, Supporting Information).



**Figure 1.** Schematic of the air-synthesis method for preparation of FAPbI<sub>3</sub> NCs.

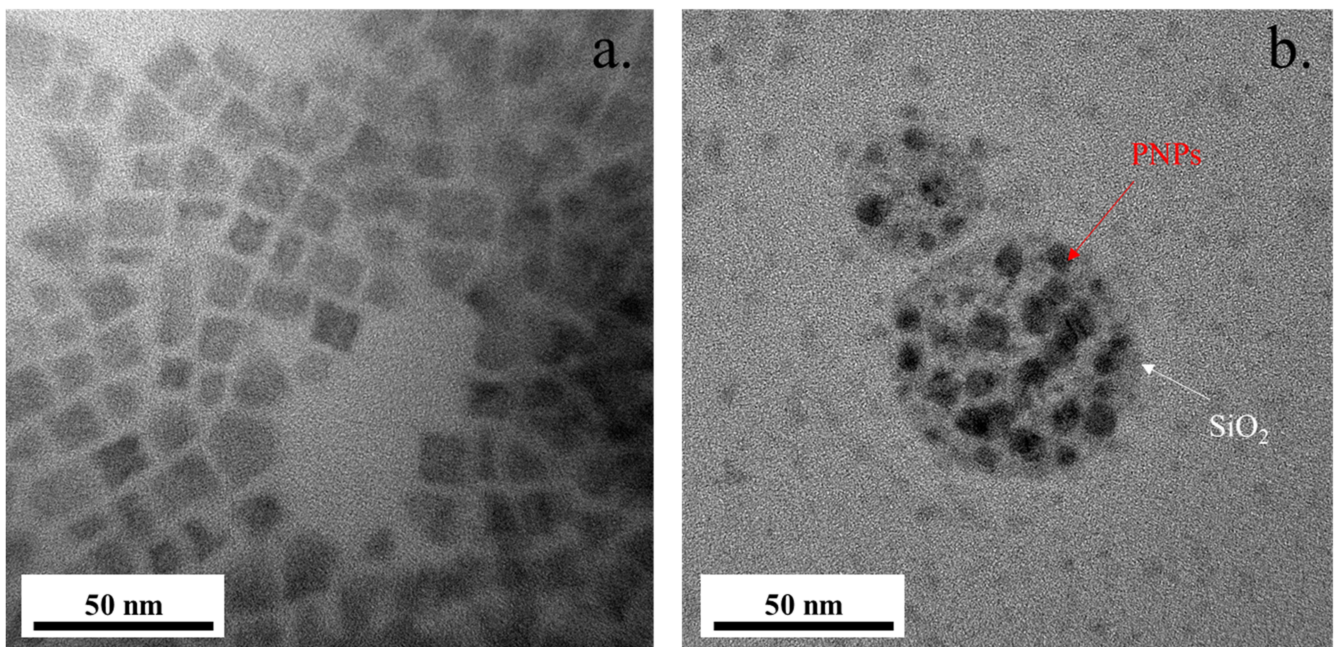
The APTES molecule provides Si–O bonds which generate the Si–O–Si ligands through hydrolysis and dehydration in the reaction to package PNPs. This protects PNPs from environmental factors [39–41]. Therefore, to verify Si–O–Si ligands on the surface of PNCs, a FTIR spectrum was used to prove the silica wrapping (Figure 2). The absorption peak at 914 and 1108 cm<sup>−1</sup> can be observed in the FAPbI<sub>3</sub> PNCs sample, which is attributed to Si–OH bonds caused by the hydrolysis condensation of APTES and asymmetrical Si–O–Si groups, respectively. These two peaks at 914 and 1108 cm<sup>−1</sup> indicate that APTES is well bonded to FAPbI<sub>3</sub> PNCs. In addition, there is a strong stretching vibration at 1710 cm<sup>−1</sup> due to C=N from FA<sup>+</sup>. The C–H stretching vibrations of CH<sub>2</sub> and CH<sub>3</sub> were detected from 2800 to 3000 cm<sup>−1</sup> [41–43].



**Figure 2.** FTIR spectra of APTES and FAPbI<sub>3</sub> NCs.

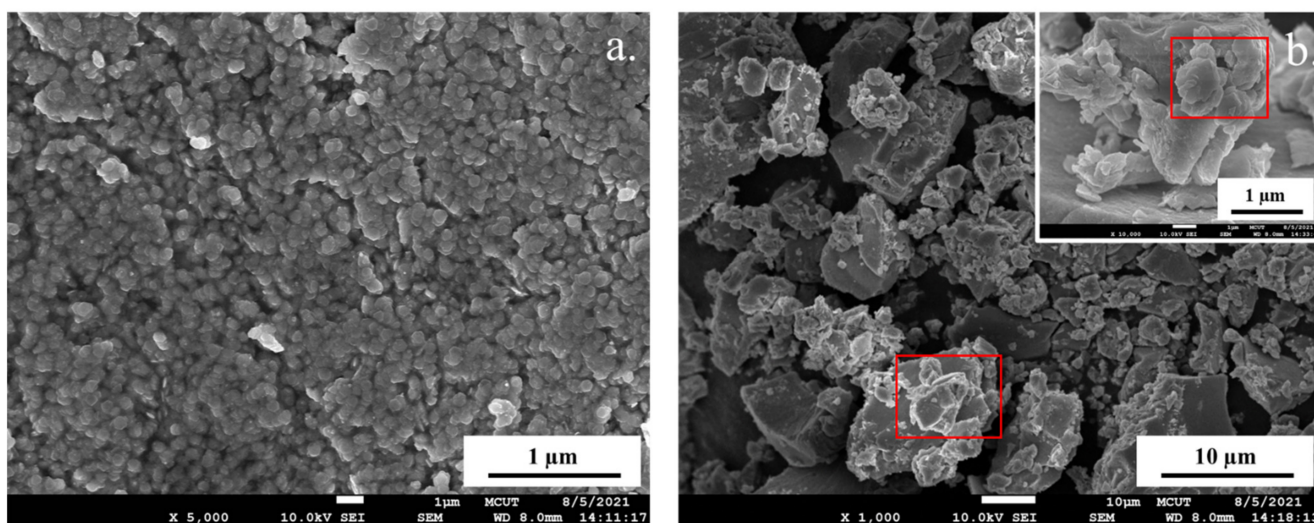
In order to verify that the PNPs embedded in silica, and confirm the real PNCs structure, the morphological features of the PNCs were observed by TEM. HRTEM images

(Figure 3a) show that the as-synthesized FAPbI<sub>3</sub> PNPs have a cubic shape. Figure 3b shows the HRTEM image of the as-prepared FAPbI<sub>3</sub> PNCs; the PNPs embedded into a shapeless material can be clearly seen, which suggests the presence of SiO<sub>2</sub> materials. These SiO<sub>2</sub> shells protect the PNPs from the influence of atmospheric moisture and oxygen [29,30]. The particle sizes have provided in Figure S1. Si and O elements can be detected by Energy dispersive spectroscopy (EDS) of Figure 3b (Figure S2), which is the evidence for the silica presence. The particle sizes of PNPs and PNCs were established to be 16.8 and 10.6 nm, respectively. The smaller size of PNCs may be due to the fact that the Si–O–Si ligands inhibit contacts between FAPbI<sub>3</sub>, leading to limited particle growth. Similar results were observed in X-ray diffraction (XRD) patterns, as shown in Figure S3. Both samples only showed the cubic phase of FAPbI<sub>3</sub>, indicating amorphous SiO<sub>2</sub>. Compared with PNPs, PNCs exhibited weaker XRD intensity, which was attributed to smaller particle size and lower perovskite particle density in the powder. Meanwhile, compared with air, the higher refractive index of SiO<sub>2</sub> can enhance the light extraction from PNCs.



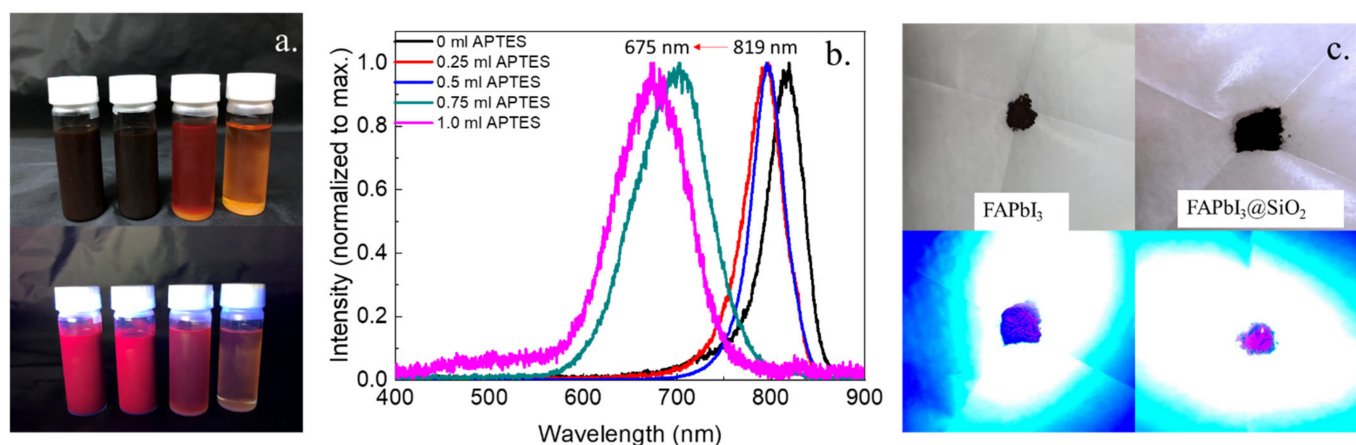
**Figure 3.** HRTEM images of (a) PNPs and (b) PNCs.

Figure 4 shows the FESEM images of the PNPs and the PNCs powders. Figure 4a shows that the larger grain size (approximately a few hundred nanometers) in the PNP powders is much greater than the TEM observation, which indicates that the PNPs aggregate without SiO<sub>2</sub> protection. The larger particles in Figure 4b were attributed to the SiO<sub>2</sub> matrix growth and network covalent solid of SiO<sub>2</sub>. Thus, the abovementioned results evidence that the PNPs and PNCs can be obtained using our simple room-temperature synthesis method.



**Figure 4.** FESEM images of (a) PNP and (b) PNC powders.

The PL spectrum of 0.25 mL APTES exhibits a narrow symmetric emission band with a peak at 795 nm, with a longer wavelength because of the scattering effect of large particles, as shown in Figure 5. However, an inadequate number of ligands leads to low PLQY (ca. 23%). When the APTES concentration increases to 0.5 mL, the highest PLQY (58.0 %) was obtained with a slight blue-shift emission. Although the emission could be further blue-shifted, the PLQY of NCs reduced. It is known that with high ligand concentrations, the rate of the reactive molecules' delivery through the silica-wrapped layer becomes slower due to the steric hindrance of Si–O–Si, resulting in smaller particles and the reduced PLQY [38]. Figure 5c shows the as-prepared PNPs and PNCs powders.



**Figure 5.** (a) Photographs of FAPbI<sub>3</sub> NCs solvent (from left to right: 0.25–1.0 mL of APTES) under room light and the UV light respectively; (b) the PL spectra of FAPbI<sub>3</sub> NCs with different amount of APTES, and (c) photographs of FAPbI<sub>3</sub> and FAPbI<sub>3</sub>NCs powders under room light and UV light.

To confirm that PNCs effectively blocks moisture and oxygen in the atmosphere, the PL spectra of the respective powders stored at approximately 26 °C with a relative humidity of approximately 75 % were measured for the different storage times. The PL intensities of the FAPbI<sub>3</sub> PNPs showed an obvious decay after 16 days, which is in agreement with previous reports [34,39,43], as shown in Figure 6a. In contrast, Figure 6b exhibits a slow decrease in PL intensity which suggests a good stability in the moist air for the FAPbI<sub>3</sub> PNCs. Furthermore, the water stability of FAPbI<sub>3</sub> PNCs was recorded by 1 mL of FAPbI<sub>3</sub> PNP and PNC solutions injecting to 2 mL of DI water. Figure 6c shows the PL intensities

of FAPbI<sub>3</sub> PNP and PNC solutions in DI water; the dark red fluorescence of FAPbI<sub>3</sub> PNPs solution decayed swiftly after 16 min in DI water. However, the FAPbI<sub>3</sub> PNC solution still showed dark red light in the DI water even after 32 min, as shown in Figure 6c. It also remained 25% of initial PL intensity after 384 min. In contrast, the FAPbI<sub>3</sub> PNCs, revealed better water stability for the FAPbI<sub>3</sub> PNCs.

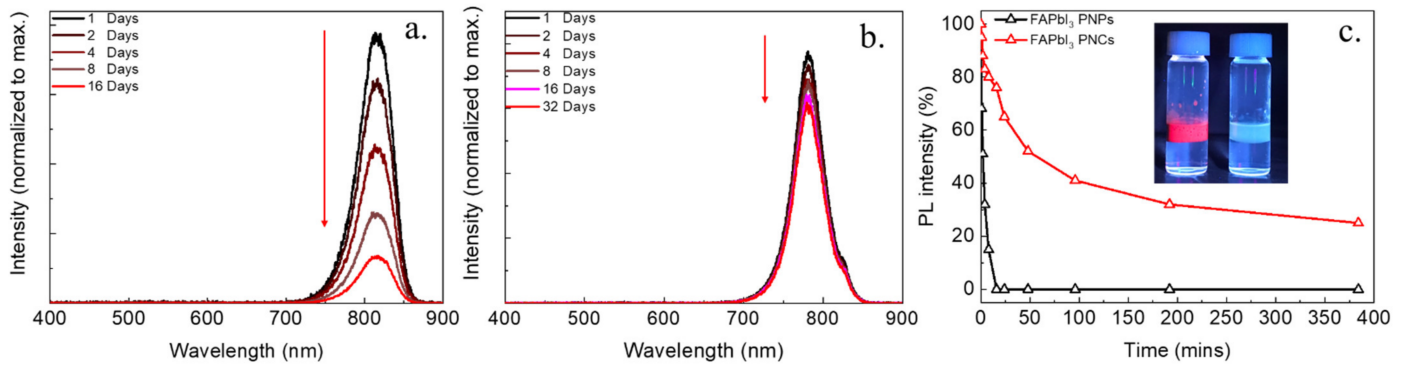


**Figure 6.** The PL spectra of FAPbI<sub>3</sub> (a) PNP and (b) PNC powders stored in air after different days; (c) the intensity of the PL peaks under the DI water as a function of times for FAPbI<sub>3</sub> PNP and PNC-dispersed solutions. The insets show the photographs of the FAPbI<sub>3</sub> PNPs and PNCs added into water after 16 min.

The NIR FAPbI<sub>3</sub> PNCs powder was coated on blue InGaN chip (wavelength = 455 nm) and NIR-LEDs were fabricated, as displayed in Figure 7a. Figure 7b shows a typical EL spectrum of NIR LEDs located at 788 nm under 2.6 V, indicating NIR emission. This may have a potential as a NIR light source to detect a blood vessel. Our results indicate that moisture-resistant and air-stability FAPbI<sub>3</sub> PNCs synthesis at room temperature is a promising material in bio-optoelectronic devices.

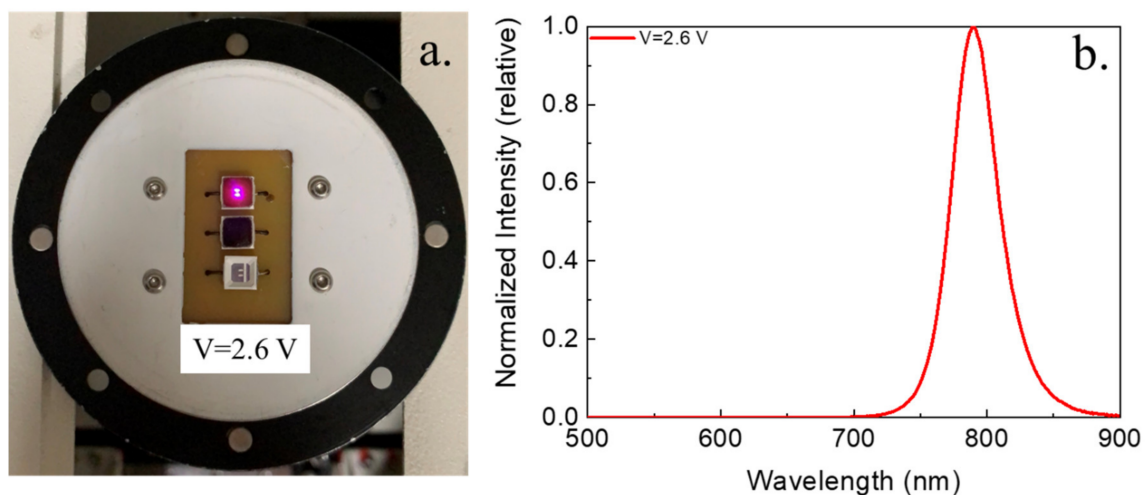


**Figure 7.** The photographs of the blue chip (455 nm) and the blue chip consisting of FAPbI<sub>3</sub> NCs under the (a) room light and (b) the NIR-LED devices EL spectrum.

#### 4. Conclusions

In conclusion, we successfully synthesized FAPbI<sub>3</sub> embedded into silica at room temperature in open air by a facile method. The air-synthesized PNCs at room temperature treatments still display high stability under ambient exposure and a narrow emission in the PL spectra. In particular, the SiO<sub>2</sub> protective layer provides high PL intensity after 32 days of storage atmosphere (28 °C) and stability in DI water. The NIR-LEDs based on the NIR-emitting FAPbI<sub>3</sub> PNCs powder coated on the blue LED have a 788 nm EL spectra.

We hope our results can be further applied in biomedical lighting applications and devices based.

**Supplementary Materials:** The following are available online at <https://www.mdpi.com/article/10.3390/bios11110440/s1>, Figure S1: The corresponding particle sizes of Figure 3 for PNPs and PNCs; Figure S2: Energy dispersive spectroscopy (EDS) of Figure 3b; Figure S3: X-ray diffractometer (XRD) patterns of FAPbI<sub>3</sub> PNP and PNC powders; Figure S4: PL intensities of the studied PNCs under (a) UV radiation (365 nm; ~0.1 W/cm<sup>2</sup>) and (b) heating treatment (100 °C) for different times.

**Author Contributions:** Conceptualization, Z.-L.T. and L.-C.C.; formal analysis, L.-W.C., C.-H.H. and Y.-T.L.; investigation, L.-W.C., C.-Y.X., Z.-M.X. and C.-C.L.; methodology, C.-H.H. and Y.-T.L.; resources, Z.-L.T. and C.-C.L.; writing—original draft, L.-C.C. All authors have read and agreed to the published version of the manuscript.

**Funding:** This work was supported by the Ministry of Science and Technology, Taiwan, under Grant No. MOST 110-2221-E-131-028-.

**Institutional Review Board Statement:** Not applicable.

**Informed Consent Statement:** Not applicable.

**Acknowledgments:** The authors would like to extend their heartfelt thanks for the use of the TEM (JEM-2100) apparatus at the Advanced Instrument Center of National Yunlin University of Science and Technology.

**Conflicts of Interest:** The authors declare no conflict of interest.

## References

1. Bekenstein, Y.; Koscher, B.A.; Eaton, S.W.; Yang, P.; Alivisatos, A.P. Highly luminescent colloidal nanoplates of perovskite cesium lead halide and their oriented assemblies. *J. Am. Chem. Soc.* **2015**, *137*, 16008–16011. [[CrossRef](#)] [[PubMed](#)]
2. Zhang, D.; Eaton, S.W.; Yu, Y.; Dou, L.; Yang, P. Solution-phase synthesis of cesium lead halide perovskite nanowires. *J. Am. Chem. Soc.* **2015**, *137*, 9230–9233. [[CrossRef](#)]
3. Li, X.; Cao, F.; Yu, D.; Chen, J.; Sun, Z.; Shen, Y.; Zhu, Y.; Wang, L.; Wei, Y.; Wu, Y. All inorganic halide perovskites nanosystem: Synthesis, structural features, optical properties and optoelectronic applications. *Small* **2017**, *13*, 1603996. [[CrossRef](#)]
4. Song, J.; Cui, Q.; Li, J.; Xu, J.; Wang, Y.; Xu, L.; Xue, J.; Dong, Y.; Tian, T.; Sun, H. Ultralarge all-inorganic perovskite bulk single crystal for high-performance visible–infrared dual-modal photodetectors. *Adv. Opt. Mater.* **2017**, *5*, 1700157. [[CrossRef](#)]
5. Sun, S.; Yuan, D.; Xu, Y.; Wang, A.; Deng, Z. Ligand-mediated synthesis of shape-controlled cesium lead halide perovskite nanocrystals via reprecipitation process at room temperature. *ACS Nano* **2016**, *10*, 3648–3657. [[CrossRef](#)] [[PubMed](#)]
6. Swarnkar, A.; Chulliyil, R.; Ravi, V.K.; Irfanullah, M.; Chowdhury, A.; Nag, A. Colloidal CsPbBr<sub>3</sub> perovskite nanocrystals: Luminescence beyond traditional quantum dots. *Angew. Chem.* **2015**, *127*, 15644–15648. [[CrossRef](#)]
7. Swarnkar, A.; Ravi, V.K.; Nag, A. Beyond colloidal cesium lead halide perovskite nanocrystals: Analogous metal halides and doping. *ACS Energy Lett.* **2017**, *2*, 1089–1098. [[CrossRef](#)]
8. Swarnkar, A.; Marshall, A.R.; Sanehira, E.M.; Chernomordik, B.D.; Moore, D.T.; Christians, J.A.; Chakrabarti, T.; Luther, J.M. Quantum dot-induced phase stabilization of  $\alpha$ -CsPbI<sub>3</sub> perovskite for high-efficiency photovoltaics. *Science* **2016**, *354*, 92–95. [[CrossRef](#)] [[PubMed](#)]
9. Ramasamy, P.; Lim, D.-H.; Kim, B.; Lee, S.-H.; Lee, M.-S.; Lee, J.-S. All-inorganic cesium lead halide perovskite nanocrystals for photodetector applications. *Chem. Commun.* **2016**, *52*, 2067–2070. [[CrossRef](#)]
10. Lv, L.; Xu, Y.; Fang, H.; Luo, W.; Xu, F.; Liu, L.; Wang, B.; Zhang, X.; Yang, D.; Hu, W. Generalized colloidal synthesis of high-quality, two-dimensional cesium lead halide perovskite nanosheets and their applications in photodetectors. *Nanoscale* **2016**, *8*, 13589–13596. [[CrossRef](#)] [[PubMed](#)]
11. Jang, D.M.; Park, K.; Kim, D.H.; Park, J.; Shojaei, F.; Kang, H.S.; Ahn, J.-P.; Lee, J.W.; Song, J.K. Reversible halide exchange reaction of organometal trihalide perovskite colloidal nanocrystals for full-range band gap tuning. *Nano Lett.* **2015**, *15*, 5191–5199. [[CrossRef](#)] [[PubMed](#)]
12. Saidaminov, M.I.; Haque, M.A.; Savoie, M.; Abdelhady, A.L.; Cho, N.; Dursun, I.; Buttner, U.; Alarousu, E.; Wu, T.; Bakr, O.M. Perovskite photodetectors operating in both narrowband and broadband regimes. *Adv. Mater.* **2016**, *28*, 8144–8149. [[CrossRef](#)] [[PubMed](#)]
13. Saidaminov, M.I.; Adinolfi, V.; Comin, R.; Abdelhady, A.L.; Peng, W.; Dursun, I.; Yuan, M.; Hoogland, S.; Sargent, E.H.; Bakr, O.M. Planar-integrated single-crystalline perovskite photodetectors. *Nat. Commun.* **2015**, *6*, 1–7. [[CrossRef](#)]
14. Yakunin, S.; Protesescu, L.; Krieg, F.; Bodnarchuk, M.I.; Nedelcu, G.; Humer, M.; De Luca, G.; Fiebig, M.; Heiss, W.; Kovalenko, M.V. Low-threshold amplified spontaneous emission and lasing from colloidal nanocrystals of caesium lead halide perovskites. *Nat. Commun.* **2015**, *6*, 1–9.

15. Fu, Y.; Zhu, H.; Schrader, A.W.; Liang, D.; Ding, Q.; Joshi, P.; Hwang, L.; Zhu, X.; Jin, S. Nanowire lasers of formamidinium lead halide perovskites and their stabilized alloys with improved stability. *Nano Lett.* **2016**, *16*, 1000–1008. [[CrossRef](#)] [[PubMed](#)]
16. Colella, S.; Mazzeo, M.; Rizzo, A.; Gigli, G.; Listorti, A. The bright side of perovskites. *J. Phys. Chem. Lett.* **2016**, *7*, 4322–4334. [[CrossRef](#)]
17. Aygüler, M.F.; Weber, M.D.; Puscher, B.M.; Medina, D.D.; Docampo, P.; Costa, R.D. Light-emitting electrochemical cells based on hybrid lead halide perovskite nanoparticles. *J. Phys. Chem. C* **2015**, *119*, 12047–12054. [[CrossRef](#)]
18. Bade, S.G.R.; Li, J.; Shan, X.; Ling, Y.; Tian, Y.; Dilbeck, T.; Besara, T.; Geske, T.; Gao, H.; Ma, B. Fully printed halide perovskite light-emitting diodes with silver nanowire electrodes. *ACS Nano* **2016**, *10*, 1795–1801. [[CrossRef](#)] [[PubMed](#)]
19. Manser, J.S.; Christians, J.A.; Kamat, P.V. Intriguing optoelectronic properties of metal halide perovskites. *Chem. Rev.* **2016**, *116*, 12956–13008. [[CrossRef](#)] [[PubMed](#)]
20. Protesescu, L.; Yakunin, S.; Bodnarchuk, M.I.; Bertolotti, F.; Masciocchi, N.; Guagliardi, A.; Kovalenko, M.V. Monodisperse formamidinium lead bromide nanocrystals with bright and stable green photoluminescence. *J. Am. Chem. Soc.* **2016**, *138*, 14202–14205. [[CrossRef](#)] [[PubMed](#)]
21. Eperon, G.E.; Stranks, S.D.; Menelaou, C.; Johnston, M.B.; Herz, L.M.; Snaith, H.J. Formamidinium lead trihalide: A broadly tunable perovskite for efficient planar heterojunction solar cells. *Energy Environ. Sci.* **2014**, *7*, 982–988. [[CrossRef](#)]
22. Song, J.; Hu, W.; Wang, X.-F.; Chen, G.; Tian, W.; Miyasaka, T. HC(NH<sub>2</sub>)<sub>2</sub> PbI<sub>3</sub> as a thermally stable absorber for efficient ZnO-based perovskite solar cells. *J. Mater. Chem. A* **2016**, *4*, 8435–8443. [[CrossRef](#)]
23. Smecca, E.; Numata, Y.; Deretzi, I.; Pellegrino, G.; Boninelli, S.; Miyasaka, T.; La Magna, A.; Alberti, A. Stability of solution-processed MAPbI<sub>3</sub> and FAPbI<sub>3</sub> layers. *Phys. Chem. Chem. Phys.* **2016**, *18*, 13413–13422. [[CrossRef](#)]
24. Binek, A.; Hanusch, F.C.; Docampo, P.; Bein, T. Stabilization of the trigonal high-temperature phase of formamidinium lead iodide. *J. Phys. Chem. Lett.* **2015**, *6*, 1249–1253. [[CrossRef](#)] [[PubMed](#)]
25. Leijtens, T.; Eperon, G.E.; Noel, N.K.; Habisreutinger, S.N.; Petrozza, A.; Snaith, H.J. Stability of metal halide perovskite solar cells. *Adv. Energy Mater.* **2015**, *5*, 1500963. [[CrossRef](#)]
26. Chen, L.-C.; Tien, C.-H.; Tseng, Z.-L.; Dong, Y.-S.; Yang, S. Influence of PMMA on all-inorganic halide perovskite CsPbBr<sub>3</sub> quantum dots combined with polymer matrix. *Materials* **2019**, *12*, 985. [[CrossRef](#)] [[PubMed](#)]
27. Huang, J.; Lei, T.; Siron, M.; Zhang, Y.; Yu, S.; Seeler, F.; Dehestani, A.; Quan, L.N.; Schierle-Arndt, K.; Yang, P. Lead-free cesium europium halide perovskite nanocrystals. *Nano Lett.* **2020**, *20*, 3734–3739. [[CrossRef](#)]
28. Huang, H.; Chen, B.; Wang, Z.; Hung, T.F.; Susha, A.S.; Zhong, H.; Rogach, A.L. Water resistant CsPbX<sub>3</sub> nanocrystals coated with polyhedral oligomeric silsesquioxane and their use as solid state luminophores in all-perovskite white light-emitting devices. *Chem. Sci.* **2016**, *7*, 5699–5703. [[CrossRef](#)]
29. Zhang, F.; Shi, Z.-F.; Ma, Z.-Z.; Li, Y.; Li, S.; Wu, D.; Xu, T.-T.; Li, X.-J.; Shan, C.-X.; Du, G.-T. Silica coating enhances the stability of inorganic perovskite nanocrystals for efficient and stable down-conversion in white light-emitting devices. *Nanoscale* **2018**, *10*, 20131–20139. [[CrossRef](#)]
30. Tang, X.; Chen, W.; Liu, Z.; Du, J.; Yao, Z.; Huang, Y.; Chen, C.; Yang, Z.; Shi, T.; Hu, W. Ultrathin, core-shell structured SiO<sub>2</sub> coated Mn<sup>2+</sup>-doped perovskite quantum dots for bright white light-emitting diodes. *Small* **2019**, *15*, 1900484.
31. Hu, X.; Zrazhevskiy, P.; Gao, X. Encapsulation of single quantum dots with mesoporous silica. *Ann. Biomed. Eng.* **2009**, *37*, 1960–1966. [[CrossRef](#)] [[PubMed](#)]
32. Wang, H.C.; Lin, S.Y.; Tang, A.C.; Singh, B.P.; Tong, H.C.; Chen, C.Y.; Lee, Y.C.; Tsai, T.L.; Liu, R.S. Mesoporous silica particles integrated with all-inorganic CsPbBr<sub>3</sub> perovskite quantum-dot nanocomposites (MP-PQDs) with high stability and wide color gamut used for backlight display. *Angew. Chem. Int. Ed.* **2016**, *55*, 7924–7929. [[CrossRef](#)]
33. Dirin, D.N.; Protesescu, L.; Trummer, D.; Kochetygov, I.V.; Yakunin, S.; Krumeich, F.; Stadie, N.P.; Kovalenko, M.V. Harnessing defect-tolerance at the nanoscale: Highly luminescent lead halide perovskite nanocrystals in mesoporous silica matrixes. *Nano Lett.* **2016**, *16*, 5866–5874. [[CrossRef](#)] [[PubMed](#)]
34. Sun, C.; Zhang, Y.; Ruan, C.; Yin, C.; Wang, X.; Wang, Y.; Yu, W.W. Efficient and stable white LEDs with silica-coated inorganic perovskite quantum dots. *Adv. Mater.* **2016**, *28*, 10088–10094. [[CrossRef](#)] [[PubMed](#)]
35. Chen, W.; Shi, T.; Du, J.; Zang, Z.; Yao, Z.; Li, M.; Sun, K.; Hu, W.; Leng, Y.; Tang, X. Highly stable silica-wrapped Mn-doped CsPbCl<sub>3</sub> quantum dots for bright white light-emitting devices. *ACS Appl. Mater. Interfaces* **2018**, *10*, 43978–43986. [[CrossRef](#)] [[PubMed](#)]
36. Zeng, F.-L.; Yang, M.; Qin, J.-L.; Teng, F.; Wang, Y.-Q.; Chen, G.-X.; Wang, D.-W.; Peng, H.-S. Ultrastable luminescent organic-inorganic perovskite quantum dots via surface engineering: Coordination of methylammonium bromide and covalent silica encapsulation. *ACS Appl. Mater. Interfaces* **2018**, *10*, 42837–42843. [[CrossRef](#)] [[PubMed](#)]
37. Yang, M.; Peng, H.-S.; Zeng, F.-L.; Teng, F.; Qu, Z.; Yang, D.; Wang, Y.-Q.; Chen, G.-X.; Wang, D.-w. In situ silica coating-directed synthesis of orthorhombic methylammonium lead bromide perovskite quantum dots with high stability. *J. Colloid Interface Sci.* **2018**, *509*, 32–38. [[CrossRef](#)]
38. Luo, B.; Pu, Y.C.; Lindley, S.A.; Yang, Y.; Lu, L.; Li, Y.; Li, X.; Zhang, J.Z. Organolead halide perovskite nanocrystals: Branched capping ligands control crystal size and stability. *Angew. Chem. Int. Ed.* **2016**, *55*, 8864–8868. [[CrossRef](#)] [[PubMed](#)]
39. Smith, A.M.; Mancini, M.C.; Nie, S. Second window for in vivo imaging. *Nat. Nanotechnol.* **2009**, *4*, 710–711. [[CrossRef](#)]
40. He, K.; Shen, C.; Zhu, Y.; Chen, X.; Bi, Z.; Marimuthu, T.; Xu, G.; Xu, X. Stable Luminescent CsPbI<sub>3</sub> Quantum Dots Passivated by (3-Aminopropyl) triethoxysilane. *Langmuir* **2020**, *36*, 10210–10217. [[CrossRef](#)] [[PubMed](#)]



41. Zhang, C.; Zhang, A.; Liu, T.; Zhou, L.; Zheng, J.; Zuo, Y.; He, Y.; Li, J. A facile method for preparing Yb<sup>3+</sup>-doped perovskite nanocrystals with ultra-stable near-infrared light emission. *RSC Adv.* **2020**, *10*, 17635–17641. [[CrossRef](#)]
42. Sun, C.; Shen, X.; Zhang, Y.; Wang, Y.; Chen, X.; Ji, C.; Shen, H.; Shi, H.; Wang, Y.; William, W.Y. Highly luminescent, stable, transparent and flexible perovskite quantum dot gels towards light-emitting diodes. *Nanotechnology* **2017**, *28*, 365601. [[CrossRef](#)] [[PubMed](#)]
43. Zhong, Q.; Cao, M.; Hu, H.; Yang, D.; Chen, M.; Li, P.; Wu, L.; Zhang, Q. One-pot synthesis of highly stable CsPbBr<sub>3</sub>@SiO<sub>2</sub> core-shell nanoparticles. *ACS Nano* **2018**, *12*, 8579–8587. [[CrossRef](#)] [[PubMed](#)]